



Investigation of temporal dynamics due to stimulated Brillouin scattering using statistical correlation in a narrow-linewidth cw high power fiber amplifier

YUSUF PANBHARWALA,¹ ACHAR V. HARISH,^{1,2} DEEPA VENKITESH,¹ JOHAN NILSSON² AND BALAJI SRINIVASAN^{1,*}

¹Department of Electrical Engineering, Indian Institute of Technology Madras, Chennai, 600036, India

²Optoelectronic Research Centre, University of Southampton, Southampton, SO18 2NU, UK

*balajis@ee.iitm.ac.in

Abstract: We experimentally investigate the dynamics of backscattered light due to stimulated Brillouin scattering (SBS) in a narrow-linewidth continuous wave (CW) fiber amplifier. We observe the onset of sharp intensity variations in the backscattered radiation as we increase the pump power, which when analyzed using Karl-Pearson's correlation coefficient reveals a distinct structure. We find that such structure is associated with the onset of stimulated Brillouin scattering (SBS) in the fiber amplifier. Moreover, at higher pump power levels we observe a periodic signature in the Karl-Pearson correlation trace that precedes an observation of kW pulses in the backscattered radiation. Based on controlled experiments, we conclude that the formation of the above kW pulses in our system is preceded by the onset of SBS.

© 2018 Optical Society of America under the terms of the [OSA Open Access Publishing Agreement](#)

1. Introduction

High power narrow linewidth sources find numerous applications such as coherent beam combining [1], light detection and ranging (LIDAR) [2, 3], and laser guide star [4, 5]. Power scaling of narrow linewidth source through fiber amplifiers is usually limited by nonlinear processes [6, 7], specifically due to the onset of stimulated Brillouin scattering (SBS) [8]. In such fiber amplifiers, the signal being amplified acts as a pump for the stimulated Brillouin scattering process resulting in a backward propagating Brillouin Stokes wave [9].

It is well known that the backscattered SBS Stokes radiation exhibits intensity variations with respect to time [10]. The intensity variation of the Stokes wave is due to the fact that the SBS process is initiated by spatially distributed and fluctuating noise source [10] within the Brillouin bandwidth. The dynamics of the SBS Stokes wave in standard single-mode silica optical fiber has been extensively studied and is reported to exhibit stochastic [11] or chaotic [12] behavior near the SBS threshold. In contrast, the SBS dynamics above the threshold in a passive fiber is also reported to have deterministic dynamical behaviors [13]. Unfortunately, the SBS dynamics in a fiber amplifier which may potentially limit the output power extracted from narrow linewidth high power amplifiers has not been as well studied.

We have recently investigated such dynamic behavior in a Yb-doped fiber amplifier operated at a pump power level near the onset of the SBS [14]. Unlike the case of passive fiber, the SBS Stokes wave in a fiber amplifier is also amplified by excited Yb-ions since the frequency separation between signal and SBS Stokes wave is only 16 GHz (at 1 μ m wavelength). This amplification of the SBS Stokes wave results in depletion of the population inversion in the Yb-doped amplifier thereby limiting the forward propagating signal power. This may lead to dramatic changes in the temporal behavior of the Stokes wave in an amplifier, which is different compared to a passive fiber. One such feature of the temporal dynamics of the SBS in an amplifier is the generation of high peak power random pulses in the fiber amplifiers. Melo et al. have reported generation of

very high peak power random pulses in the backward direction when a pulsed signal is amplified in a fiber amplifier [15]. These high peak power (kW-level) pulses generated in the backward direction can potentially damage the components in the upstream amplifier and master oscillator stages. A. V Kiryanov et al. have also reported similar generation of kW pulses in a fiber laser cavity [16]. In their work, they also discuss the possible role of SBS in the initiation of the kW-level self pulsing. However, they do not prescribe any systematic methodology to track the onset of such kW pulses [16]. In [17], Tang and Xu reports the generation of random Q-switched pulses with high peak power in a fiber laser. In this work, random cavities are formed along the fiber due to the Rayleigh scattering arising from the intrinsic micro-scale refractive-index irregularities of fiber cores. The Q-factor of the cavity is rapidly increased by stimulated Brillouin scattering resulting in high peak power pulses. Occurrence of kW level pulses with highly varying amplitude levels are also described by Hanzard et. al. which are attributed to SBS in a fiber laser [18].

In this article, we report the observation of SBS temporal dynamics in a narrow linewidth, high power CW Yb-doped fiber amplifier. We observe the SBS backscattered power for different amplifier power levels. We analyze this SBS temporal dynamics by calculating Karl- Pearson's correlation coefficients. We find that tracking the pattern of correlation coefficient is a good indicator for the onset of random high peak power (kW level pulses). Through the controlled experiments discussed in this paper, we correlate the generation of kW level pulses with time dynamic behavior of SBS generation. We further compare the temporal dynamics of the high power fiber amplifier to that of a passive fiber and conclusively establish the origin of random high-power intensity variations in the case of an amplifier.

2. Experimental setup

Our experimental setup comprises an all-fiber three stage master oscillator power amplifier (MOPA) as shown in Fig. 1. Each stage is separated by an isolator with >28 dB isolation. The seed is a narrow linewidth CW distributed feedback (DFB) semiconductor diode laser emitting at 1064 nm, whose full-width at half-maximum (FWHM) linewidth is measured to be ~100 kHz using the delayed self-heterodyne method [19]. The output of the seed laser is fed to a pre-amplifier (FA1) through a phase modulator (EOspace, PM-0S5-10-PFA-PFA-106) followed by an isolator. The pre-amplified output is further amplified to 2 W power level using a power amplifier stage (FA2) comprising 5 m of Yb-doped double-clad fiber (Nufern fiber LMA-YDF-10/130-VIII, core/clad diameter -10/130 μm) and cladding-pumped at 915 nm. The output of FA2 is further amplified in a third amplifier stage (FA3), which is built with 3.3 m of Yb-doped double-clad fiber (Nufern fiber LMA-YDF-15/130-VIII, core/clad diameter 15/125 μm) and cladding-pumped at 975 nm. The output port of the doped fiber is angle cleaved at $\sim 12^\circ$ to minimize the coupling of reflections back into the fiber. Tap ports integrated with the isolator at each stage are used to monitor the forward and backward propagating signal as shown in Fig. 1. Specifically, the tap monitoring the backscattered radiation at each isolator is primarily used to observe the onset of SBS in the subsequent amplifier stage.

The output from the tap ports is also used to carry out time domain measurements. We use an InGaAs receiver (Thorlabs - PDB470C) with a bandwidth of 400 MHz and a digital storage oscilloscope (Lecroy 10 GS/sec, Model No. 104MXs-B) to collect the temporal traces which are stored and then post-processed in a computer.

3. Experimental results

Figure 2 shows output signal power (on the left axis) and the back-scattered SBS Stokes power (on the right axis) for different FA3 pump powers. The variation of SBS Stokes power shows an abrupt change after 37 W of pump power. As we amplify the signal in FA3 and monitor its backscattered instantaneous power, we observe low intensity fluctuations that are initiated at an

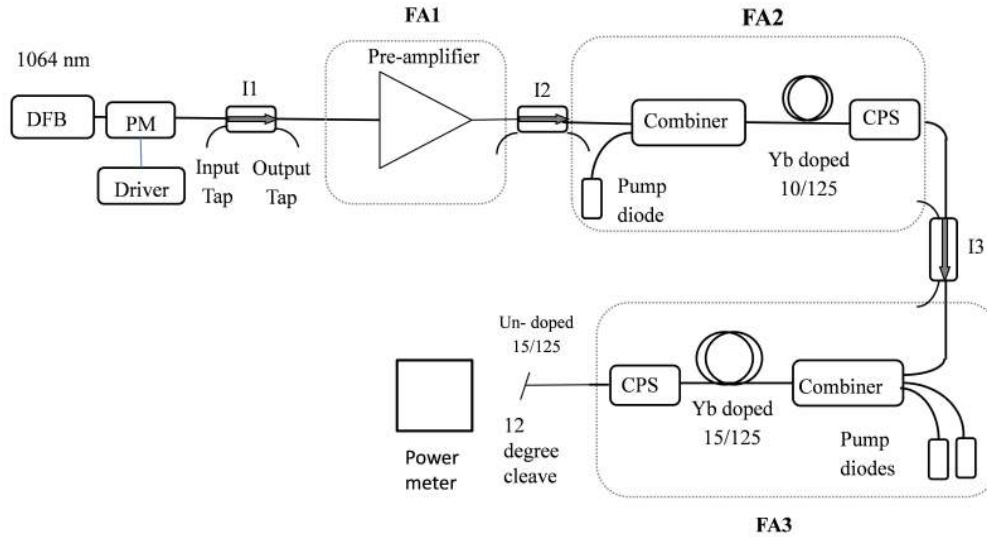


Fig. 1. Schematic of the master-oscillator power amplifier (MOPA) showing three stages of signal amplification, i.e. fiber amplifier 1 (FA1), fiber amplifier 2 (FA2) and fiber amplifier 3 (FA3). DFB: distributed feedback laser, PM: phase modulator, I: Isolator, Yb: Ytterbium, CPS: cladding pump stripper.

output signal power of 18 W. Such intensity fluctuations are consistent with those reported earlier for passive optical fibers [13] and are attributed to the onset of SBS. As previously discussed by Harrison et. al. the backscattered light due to SBS exhibits periodic intensity fluctuations for a passive fiber [13]. An autocorrelation can be a useful tool for identifying and quantifying the periodicity of the traces captured. We calculate the Karl Pearson's correlation coefficient (A_L) for the captured time trace of length 1 ms (much greater than the FA3 transit time of ~ 50 ns), which measures the autocorrelation and gives a number that varies between -1 and +1 [20]. The auto-correlation co-efficient is calculated as

$$A_L = \frac{\sum_{r=1}^{N-L} (x_r - \bar{x})(x_{r+L} - \bar{x})}{\sum_{r=1}^N (x_r - \bar{x})^2} \quad (1)$$

where x_r is the sample value, x_{r+L} is the sample value after a lag of L samples, N is the total number of samples in the temporal trace, and \bar{x} is the mean value of all the samples of the temporal trace.

Next, we show the time domain traces captured in the backward direction in Fig. 3(a)-3(c) for different output signal powers and plot the corresponding correlation co-efficient versus the time lag L in Fig. 3(d) to analyze the backscattered signal. The correlation coefficient is calculated for the time traces captured for 1 ms duration. However we have plotted the time traces for 20 μ s duration in Fig. 3(a), 3(b) and 3(c) from the 1 ms data for the purpose of clear visual representation. At low output signal powers before the onset of SBS, the time trace does not show any well-defined intensity variation as seen in the Fig. 3(a) for 12 W output signal power. The corresponding Karl Pearson correlation coefficients (A_L) plotted in Fig. 3(d) exhibits a peak only at zero lag. As the output signal power is increased to 18 W, we observe sharp variations in the backscattered intensity as shown in Fig. 3(b). As mentioned earlier, such sharp variations are consistent with the onset of SBS [13]. Interestingly, the sharp variations in the time domain trace

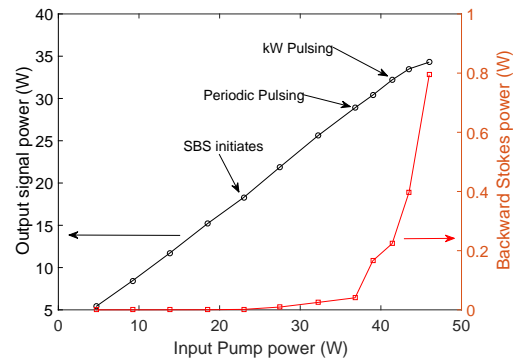


Fig. 2. Plot of the output signal power (left axis) and SBS Stokes power (right axis) vs input pump power (FA3) with marking of the initiation of SBS and kW pulsing.

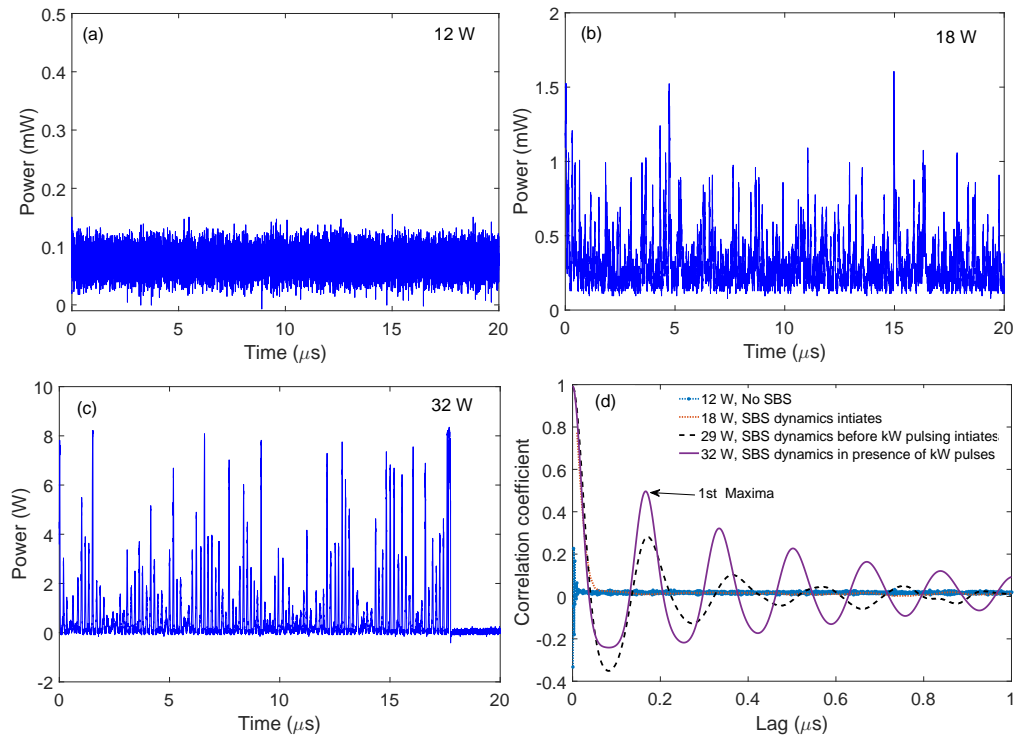


Fig. 3. Plot of the temporal trace of the backscattered light captured with a fast photodiode for different output signal powers of (a) 12 W, (b) 18 W, and (c) 32 W, (d) plot of Karl Pearson's co-efficient vs. the lag.

manifests itself as finite width of main peak in the correlation trace plotted in Fig. 3(d) [11]. In fact, if we plot the width of the main peak in the correlation trace as a function of the output signal power as shown in Fig. 4 we see an abrupt change at 18 W of signal power. This indicates the onset of SBS at a output signal power level much lower than the level at which the average Stokes backscattered optical power exhibits an abrupt change (~ 30 W).

As we further increase the signal power to 29 W, we observe that the SBS dynamics start showing periodic behavior, which is confirmed by the corresponding autocorrelation trace in

Fig. 3(d). The SBS dynamics for 32 W of signal power plotted in Fig. 3(c) shows a relatively "quiet" region (beyond 18 μs in Fig. 3(c)) where the sharp intensity variations are absent. This observation, which coincides with a sudden reduction and subsequent recovery of output power in forward direction is explained in more detail below. The corresponding correlation coefficients are plotted in Fig. 3(d) which once again confirms the periodic temporal behavior of the intensity variations.

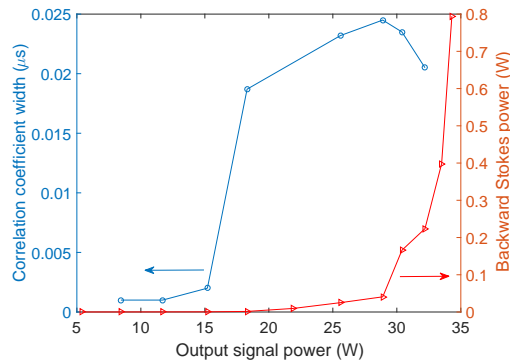


Fig. 4. Plot of correlation coefficient 3-dB width (left axis) and SBS Stokes power (right axis) vs output signal power (FA3).

Moreover, at 32 W output signal power, we observe high peak power pulses with varying peak amplitude occurring in the backward direction at random intervals along with the regular SBS induced periodic amplitude variation. Note that the high peak power random pulses are not observed at signal power of 29 W where the periodic behavior of SBS dynamics is initiated (refer Fig. 3(d)). To measure the peak power of these random high peak power pulses, we introduced optical attenuation for the backscattered light. After optical attenuation, the periodic SBS dynamics are below the detector sensitivity in the temporal trace and only the high peak power pulses are captured in the oscilloscope as shown in the Fig. 5(a). We observe a mean pulse separation time of 55 μs over 1 ms timescale, FWHM pulsewidth of 10 ns and an average peak power of 1.12 kW. The inset of Fig. 5(a) shows the time domain plot without the optical attenuation. In the inset we see a high peak power pulse (one of these kW pulses measured) saturating the detector. After the kW pulse, the SBS dynamics are muted for 10s of μs as shown in the inset of Fig. 5(a). This silent regime is attributed to a depletion of the gain in the Yb-doped fiber amplifier due to the kW pulse, and is followed by a gradual gain recovery phase. Such a hypothesis is corroborated by the observation of a sudden decrease in the FA3 output power followed by a recovery over the same timescale (10s of μs).

We also measured the kW pulses for higher pump powers and observed that its repetition rate and the peak power increases. Such an observation is explained by the faster gain recovery due to higher pumping rates [17]. Figure 5(b) illustrates the spectrum of the backscattered radiation for output signal power levels of 29 W, 32 W, and 34 W respectively. Since the pulses are occurring at random times with random amplitudes, we used the maximum hold option in the optical spectrum analyzer (Agilent 86140B) to capture the spectra at a resolution bandwidth (RBW) of 1 nm. We observe spectral peaks at ~ 1120 nm and ~ 1180 nm, which correspond to the first and second order Stokes component of stimulated Raman scattering (SRS). The theoretically calculated threshold for the SRS in FA3 is 4 kW, where we use a Raman gain coefficient of 50 fm^2/W , the effective area of $78.5 \mu\text{m}^2$ and amplifier effective length of 5 m. Although we are not observing peak power levels corresponding to the SRS threshold in our kW pulses, we believe that we are quite close to that value.

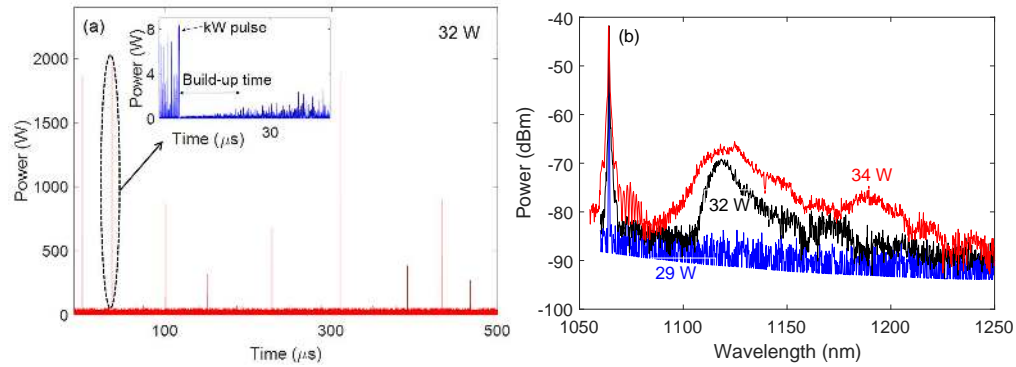


Fig. 5. (a) Plot of backscattered kW peak power pulses against time, the inset shows the zoomed in plot of (a) showing the detector saturation due high peak power and (b) backward spectrum captured with resolution bandwidth of 1 nm showing the increase in the Raman scattering with increasing output signal power.

4. Discussion

To investigate the role of SBS dynamics in the formation of kW pulses, we systematically increase the power level corresponding to the onset of SBS by broadening the seed laser linewidth. The linewidth broadening is carried out through an external phase modulator. We drive the phase modulator with a simple sinusoidal electrical signal with a fixed frequency of 40 MHz and vary the phase modulation depth (γ) by controlling the applied voltage [21]. Increasing the modulation depth increases the number of spectral lines generated at the output of phase modulator and hence broadens the signal linewidth.

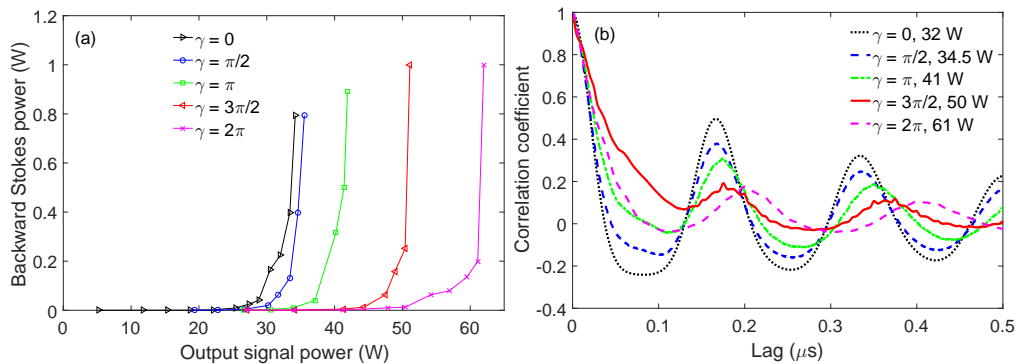


Fig. 6. (a) Plot of the backscattered SBS Stokes power against the output signal power for different modulation depths and (b) Karl Pearson correlation coefficient (A_L) plotted against the time lag for different output signal power at which the kW peak power pulses are initiated for different modulation depths.

We see no significant changes in the temporal characteristics with signal linewidth broadening except for the change in the power levels at which the SBS initiates (seen in Fig. 6(a)) and power at which the random high peak power pulse appears. Figure 6(b) plots the Karl Pearson correlation coefficient of the SBS dynamics at the output signal power where kW pulses are initiated (without optical attenuation of the backscattered power) for different modulated depths. We clearly observe that the kW pulses are generated beyond the power level at which the SBS Stokes shows periodic behaviour (as seen from autocorrelation plots). Since we now establish

that the precursor for the appearance of kW pulses is a periodic behavior in the autocorrelation trace, tracking such periodicity and adopting appropriate strategies while power scaling will prevent the catastrophic damage to the upstream components due to these kW pulses.

We have also observed similar generation of random high peak power pulses in the backward direction due to SBS in FA2 when its output power level was boosted to 3.3 W. Even in FA2 we observe similar periodic behaviour in SBS dynamics which then leads to generation of random high peak power pulses (note that FA2 was operated at ~ 2 W output power when it was used to seed FA3 and hence there was no sign of SBS), albeit the pulse peak powers are in the range of 40 to 50 W due to lower gain available in FA2.

Next, we compare the dynamics of the backscattered light due to SBS in a passive fiber to the active fiber amplifier. We splice 18 m of HI-1060 passive fiber ($6 \mu\text{m}$ core dia.) at the output of the FA2 after the isolator. The fiber end facet is angle cleaved at an angle of $\sim 12^\circ$. We then plot the output signal power against the input signal power as shown in the Fig. 7(a) (left axis) and the backscattered SBS Stokes power versus the input signal power (on the right axis). The temporal trace of the backscattered light due to SBS is plotted in the Fig. 7(b) and 7(c) for input signal powers of 2 W and 2.4 W respectively. The corresponding Karl Pearson coefficient versus the time lag is plotted in Fig. 7(d). We clearly see oscillatory behavior corresponding to the periodic intensity variations in the backscattered SBS Stokes radiation for an input signal power level of 2.4 W. However, we do not see the random high peak power pulses in the passive fiber even when we go to high SBS reflectivities (ratio of backward stokes power to input signal power)

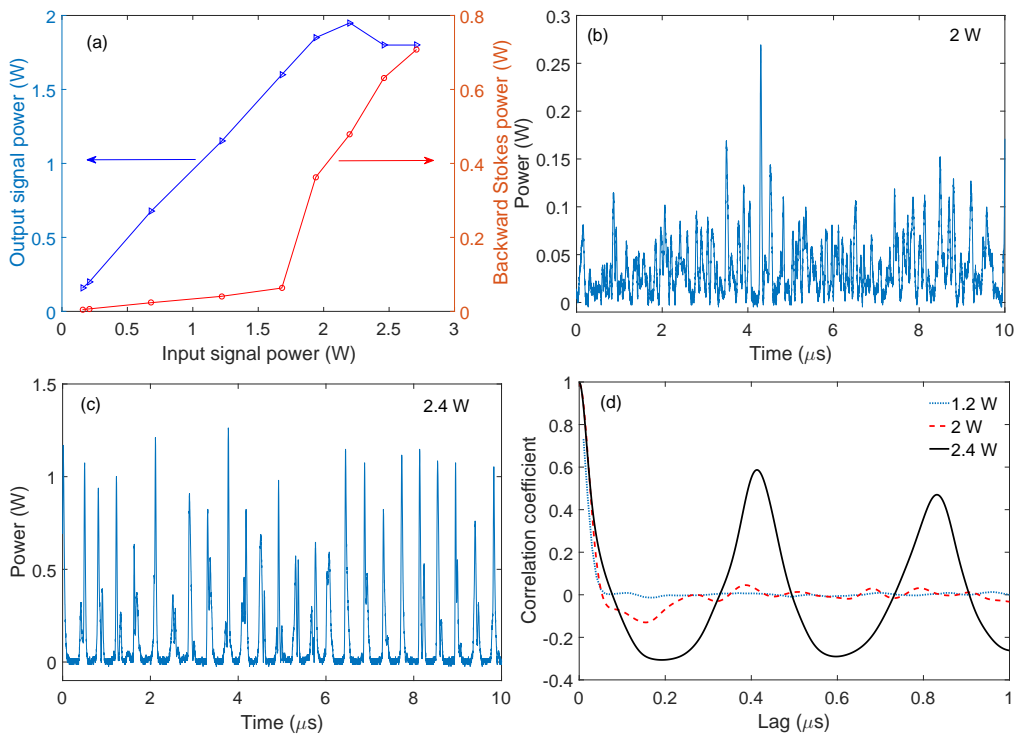


Fig. 7. (a) Plot of the output signal power (left axis) and backscattered SBS Stokes power (right axis) against the input signal power (Brillouin pump power) for a 18 m long Hi1060 fiber and (b) Temporal trace of the backscattered power in the passive fiber at (b) 2 W and (c) 2.4 W, and (d) Karl Pearson correlation coefficient plotted against the time lag for different input signal power levels.

like 25% [8]. This confirms that the high peak power random pulsing occurs only in active fiber amplifiers due to presence of Yb-gain.

Random kW pulses were also reported in [16], where the authors see high peak power random Q-switched pulsing in a Yb-doped fiber laser. Unlike our setup, [16] has a cavity that is built using fiber Bragg gratings whose Bragg wavelength determines the lasing peak. Tang and Xu [17] also reports the generation of such random kW pulses from a cavity formed only by Rayleigh scattering at one end of the gain fiber. In both these cases, the cavity Q value is increased drastically due to the onset of SBS and leads to the generation of high peak power pulses due to the presence of Yb gain. Our results are not only consistent with the above mechanism, but also provides a clear pathway to track the onset of the kW pulsing behavior.

Another important aspect of the correlation plots of the SBS Stokes is the lag value at which the first maxima occurs which corresponds to the periodicity of the temporal intensity variations. For passive fibers, it is reported that the periodicity of the intensity variations due to SBS corresponds to $2 T_r$, where T_r is the transit time across the passive fiber [22]. We have observed a similar periodicity for passive fiber length of 40 m and 520 m. However, when we investigate the same for a 18 m long passive fiber, the time lag for the first maxima is observed to be ~ 400 ns which is greater than $4T_r$. We observe similar results for the fiber amplifiers (FA3 and FA2), suggesting that there is a dependence of the periodicity on the length of the fiber which needs a more detailed investigation.

5. Conclusion

We have experimentally investigated dynamics of backscattered light due to SBS in a narrow line and high power CW optical fiber amplifier. We use Karl Pearson correlation coefficient to analyze the backscattered SBS Stokes wave. By observing the width of the main peak in the correlation trace, we show that the onset of SBS can be tracked at a much lower power level compared to a corresponding measure based on the average Stokes backscattered power. As we increase the signal power in our fiber amplifier, we observe a periodic behavior of the SBS Stokes wave followed by the generation of kW-level pulses. Through controlled experiments, we establish that the onset of high peak power random pulses is preceded by the onset of SBS in our fiber amplifier. We find that the threshold signal power for random high peak power pulsing is pushed to a higher value when the linewidth of the DFB source is chirped using an external phase modulator. Similarly, when we investigate the backscattered radiation from a passive fiber at high SBS gain, we do not observe any high peak power random pulsing. This suggests that Brillouin dynamics in the presence of Yb-gain plays an important role in the generation of these random high peak power pulses. Work is in progress to develop a numerical model that can describe the dynamics in an optical fiber amplifier combining the SBS model as well as the rare-earth doped fiber amplifier.

Funding

Asian Office of Aerospace Research and Development (AOARD) (FA2386-16-1-4077); Ministry of Electronics and Information Technology (MeitY, Govt. of India) (Visvesvaraya PhD scheme); Department of Science and Technology (DST, Govt. of India) (Inspire faculty scheme).

Acknowledgments

The authors would like to acknowledge Aditi Ghosh for technical discussions.

References

1. R. Su, P. Zhou, X. Wang, Y. Ma, and X. Xu, "Active coherent beam combination of two high-power single-frequency nanosecond fiber amplifiers," *Opt. Lett.* **37**, 497-499 (2012).
2. J. Shi, G. Li, W. Gong, J. Bai, Y. Huang, Y. Liu, S. Li, D. Liu, "A lidar system based on stimulated Brillouin scattering," *Appl. Phys. B* **86**, 177-179 (2007).
3. R. Su, P. Zhou, X. Wang, H. Laj, and X. Xu, "Nanosecond pulse pumped, narrow linewidth all-fiber Raman amplifier with stimulated Brillouin scattering suppression," *J. Opt.* **16**, 015201 (2014).
4. L. R. Taylor, Y. Feng, and D. B. Calia, "50W CW visible laser source at 589nm obtained via frequency doubling of three coherently combined narrow-band Raman fibre amplifiers.," *Opt. Express* **18**, 8540-8555 (2010).
5. C. X. Yu, S. J. Augst, S. M. Redmond, K. C. Goldizen, D. V. Murphy, A. Sanchez, and T. Y. Fan, "Coherent combining of a 4 kW, eight-element fiber amplifier array," *Opt. Lett.* **36**, 2686-2688 (2011).
6. R. G. Smith, "Optical Power Handling Capacity of Low Loss Optical Fibers as Determined by Stimulated Raman and Brillouin Scattering," *Appl. Opt.* **11**, 2489-2494 (1972).
7. A. Liem, J. Limpert, H. Zellmer, and A. Tajnnermann, "100-W single-frequency master-oscillator fiber power amplifier.," *Opt. Lett.* **28**, 1537-1539 (2003).
8. A. Kobayakov, M. Sauer, and D. Chowdhury, "Stimulated Brillouin scattering in optical fibers," *Adv. Opt. Photon.* **2**, 1-59 (2010).
9. D. J. Richardson, J. Nilsson, and W. A. Clarkson, "High power fiber lasers: current status and future perspectives [Invited]," *J. Opt. Soc. Am. B* **27**, B63-B92 (2010).
10. R. W. Boyd, K. Rzaewski, and P. Narum, "Noise initiation of stimulated Brillouin scattering," *Phys. Rev. A* **42**, 5514-5521 (1990).
11. A. L. Gaeta and R. W. Boyd, "Stochastic Dynamics of Stimulated Brillouin Scattering in an Optical Fiber," *Phys. Rev. A* **44**, 3205-3209 (1991).
12. R. G. Harrison, J. S. Uppal, A. Johnstone, and J. V. Moloney, "Evidence of chaotic stimulated Brillouin scattering in optical fibers," *Phys. Rev. Lett.* **65**, 167-170 (1990).
13. R. G. Harrison, D. Yu, W. Lu, and P. M. Ripley, "Chaotic stimulated Brillouin scattering: theory and experiment," *Physica D: Nonlinear Phenomena* **86**, 182-188 (1995).
14. Y. Panbiharwala, A. Ghosh, J. Nilsson, D. Venkitesh, and B. Srinivasan, "Experimental investigation of the onset of modulation instability as a precursor for the stimulated Brillouin scattering in Yb-doped fiber amplifiers," *Proc. SPIE* **10512**, 105122X (2018).
15. M. Melo, M. O. Berendt, and J. M. Sousa, "Destructive random backscattering pulses showing Brillouin signature in MOPA fiber laser systems," *Proc. SPIE* **8601**, 86011P (2013).
16. A. V Kiryanov, Y. O. Barmenkov, and M. V Andres, "An experimental analysis of self-Q-switching via stimulated Brillouin scattering in an ytterbium doped fiber laser," *Laser Phys. Lett.* **10**, 055112 (2013).
17. Y. Tang and J. Xu, "A random Q-switched fiber laser," *Scientific Reports* **5**, 9338 (2015).
18. P. Hanzard, M. Talbi, D. Mallek, A. Kellou, H. Leblond, F. Sanchez, T. Godin and A. Hideur, "Brillouin scattering-induced rogue waves in self-pulsing fiber lasers," *Scientific Reports* **7**, 45868 (2017).
19. D. Derickson, *Fiber Optic Test and Measurement* (Prentice Hall PTR 1998).
20. W. H. Press, S. A. Teukolsky, B. Flannery, and B. P. Flannery, *Numerical Recipes in C* (Cambridge University 1992).
21. C. Zeringue, I. Dajani, S. Naderi, G. T. Moore, and C. Robin, "A theoretical study of transient stimulated Brillouin scattering in optical fibers seeded with phase-modulated light," *Opt. Express* **20**, 21196-21213 (2012).
22. E.P. Ippen and R.H. Stolen, "Stimulated Brillouin scattering in optical fibers," *Appl. Phys. Lett.* **21**, 539 (1972).